

Determining Decadal Mean Deep Zonal Flows from Synoptic Observations in the South Atlantic

*A.M. Thurnherr, *K.G. Speer, †A.-M. Treguier

**Dept. of Oceanography, FSU, Tallahassee, FL; †LPO, IFREMER, Brest.*

Submitted for publication in Science

September 5, 2002

The deep oceanic circulation plays an important role in climate, transporting heat and greenhouse gases. Velocity measurements in the western basin of the South Atlantic have revealed a flow field that is primarily zonal at 2500 and at 4000 m. Here we show that the observations are representative of a quasi-steady state, which is consistent with tracer distributions but not with several published hydrographic analyses. The main reason for this is the violation of a fundamental assumption of “standard” oceanographic methods, caused by the baroclinic nature of the large-scale slowly time-varying flow field, which is as strong as the mean circulation.



The oceanic circulation transports numerous dissolved and particulate substances and is therefore important in a variety of contexts, such as economic geology and biogeography. Because of the ocean's capacity for storing and transporting large amounts of heat and greenhouse gases it plays an pivotal role in climate (1, 2). While the near-surface currents are generally much stronger than those in the deep in-

terior of ocean basins the corresponding transports are similar because of the large vertical scales associated with the deep flows. The most commonly used method for determining the deep currents consists in adjusting reference velocities of geostrophic profiles (1), usually calculated from synoptic hydrographic data. In most cases it is unclear to what extent the resulting deep circulations are representative for longer time scales, implying that little is known about the mean deep circulations in the interior of most ocean basins. In the Brazil Basin in the South Atlantic the deep velocity field has been observed directly with floats and current meters (3, 4). It is dominated by zonal flows, which are partially consistent with an analysis based on tracer distributions (5) but inconsistent with hydrographic analyses (6–9). Here we show why this is the case.

Along the pathways of oceanic flows the concentrations of dissolved and particulate tracers vary because of non-conservative processes including chemical reactions, dissolution and precipitation of particles, horizontal and vertical mixing, etc. The resulting spatial property gradients can be used to constrain the oceanic circulation. Examples include

mean flows inferred from basin-scale hydrothermal helium plumes in the Pacific ocean (12) and from tracer fields in the western South Atlantic (5, 7, 13). At the level of North Atlantic Deep Water (NADW) the horizontal distribution of bias-corrected oxygen data (10) collected in the Brazil Basin between 1983 and 1995 is characterized by alternating zonal tongues (Figure 1); the corresponding salinity and silicate fields show the same patterns (10). At the resolution permitted by the measurement accuracy and station spacing of the 1925–1927 Meteor data set (13) the oxygen pattern has not changed significantly during more than half a century.

Inspection of the tracer fields at the NADW level in the Brazil Basin reveals that the main patterns extend across multiple data sets, implying persistence. Large-scale tracer tongues are often interpreted as evidence for a quasi-steady circulation, but they can be maintained in principle without Eulerian mean flows, i.e. by turbulent Reynolds fluxes alone (14). A combination of advective and eddy-diffusive fluxes provides the most plausible mechanism for maintaining persistent tracer tongues (15) but since horizontal and vertical eddy fluxes are not well known, the in-

terpretation of tracer patterns is generally ambiguous (7).

Velocities derived from float observations (3, 4) reveal a close correspondence between the tracer tongues and the flow field in the Brazil Basin (Figure 1). The data strongly suggest that the mean flow is along the tongues' axes, supporting the central assumption of Wüst's core-layer method (13). (The corresponding patterns in uncorrected tracer data (5, 6, 16) do not line up closely enough with the velocity field to rule out flow around the tongues.) At lower latitudes the correspondence between the velocities and the tracers is less close but we note that the meridional separation of the floats may not adequately resolve the smaller scales of the patterns there. The NADW tongues in the Brazil Basin apparently emanate from the western boundary and bias-corrected tracer maps covering the entire South Atlantic (10) show little evidence for NADW crossing the crest of the Mid-Atlantic Ridge. Hydrographic and tracer-dispersal observations suggest predominantly southward flow along the western ridge flank near 20°S (17), i.e. in the region of strong zonal oxygen gradients.

The float-derived velocity observations are neither consistent with a circulation analysis based purely on tracer fields (Tsuchiya et al. (5) infer counterclockwise flow around the high-oxygen tongue centered at 22°S) nor, in our opinion, with geostrophic velocities derived from a hydrographic section at 25°W (8, 16, 18). Our assessment is somewhat subjective, as there is agreement between tracers and the synoptic geostrophic velocities in parts of the domains of all cited studies. Many of the inferred synoptic zonal velocity cores are offset from the corresponding tracer tongues and at some latitudes the analyses (based on the same data) disagree on the directions of the flow. Therefore, we infer that the relationship between tracer fields and synoptic geostrophic velocities remains inconclusive. This uncertainty casts some doubt on the assumption that the mean deep oceanic circulation can be determined from geostrophic velocities derived from synoptic hydrographic sections (1). We will now show that the problem lies in the spatial characteristics of the large-scale time-varying flow field, which is comparable in magnitude to the mean circulation and has vertical structure that cannot be accounted for with reference-velocity adjust-

ments. Furthermore, the horizontal scales of the unsteady and steady flow components are similar, precluding separation by spatial averaging.

The upper two panels of Figure 2 show meridional density gradients observed in 1994 at 19°W (WOCE A15) and in 1989 at 25°W (Hydros 4, aka. SAVE 6, aka. WOCE A16 (5)). In order to remove the effects of mesoscale eddies and internal waves the gradients are calculated in 7.25°-wide meridional windows (8). The thermal wind equation (19) implies that the meridional density gradients at a given latitude are proportional to the vertical shear of the geostrophic zonal velocities. The similarity of the patterns observed in the two sections is striking and unexpected, especially at depth. The time lag between the observations suggests that the patterns are the signatures of quasi-steady mean flows, and the zonal distance implies that the mean zonal flows are zonally coherent over at least 600 km. The patterns are qualitatively consistent with horizontally and vertically banded velocity cores of alternating directions. To our knowledge this is the first clear hydrographic evidence showing the spatial structure of a weak mean circulation in the interior of a deep ocean basin.

In order to determine the zonal geostrophic velocity field from meridional density gradients the thermal-wind equation has to be integrated vertically. The reference velocities (integration constants) must be determined using additional constraints (1), and different methods applied to the same data generally yield different velocity fields (8, 18). A comparison of the meridional density gradients (Figure 2) with geostrophic velocities derived from the 25°W section (5, 18) reveals that the high vertical structure apparent in the density gradients is largely obscured in the corresponding geostrophic velocities. The same observation holds at 19°W. The synoptic geostrophic velocities are therefore dominated by lower modes than those apparent in the meridional density-gradient patterns. (Differentiation emphasizes the high frequencies.) Below the westward velocities associated with the subequatorial and subtropical gyres (18) the synoptic geostrophic velocity fields at 19° and 25°W are qualitatively and quantitatively different, and it is in the low modes that the main differences are found. The typical meridional extent of the patterns in the geostrophic-velocity differences is several hundred kilometers, similar to the

meridional scales of the density-gradient patterns. While it is not possible to separate temporal from spatial effects in the available hydrographic data the zonal coherence of the tracer fields between 19° and 25°W in the southern Brazil Basin (Figure 1) suggests that the differences between the two hydrographic sections are primarily temporal rather than spatial.

In order to separate temporal and spatial effects we use output from a 1/6° general circulation model (11), spun up to dynamic equilibrium (20). The meridional density gradients above ≈ 4000 m in a 5-year-averaged model output (bottom panel of Figure 2) are qualitatively and quantitatively similar to the observations. Below 4000 m the model circulation is unrealistic because of insufficient inflow of Antarctic Bottom Water into the Brazil Basin. The time-averaged model density gradients at 19° and 25°W are nearly indistinguishable, consistent with the data-based inference that the observed density-gradient patterns are signatures of zonally coherent quasi-steady mean flows.

The similarity between the observed and modeled density gradients suggests that the mean zonal cir-

ulation in the numerical model is realistic. In order to analyze the flow field, the model velocities (Figure 3) are meridionally smoothed using a 2.5° Gaussian filter, which has a scale dependence similar to the 7.25°-wide linear regressions used for the gradient calculations. The temporally averaged model velocities at 2500 m (top panel) are nearly everywhere qualitatively and quantitatively consistent with the float velocities (Figure 1). (The primary exception is the narrow oxygen minimum near 7°S, which is not associated with westward flow in the model.) In accordance with our data-based inference, the vertical structure of the time-varying zonal flow field in the model (bottom panel) is dominated by lower modes than those of the mean circulation; it is not barotropic, however. Below the near-surface westward flow associated with the subequatorial and subtropical gyres (18) the time-varying and the mean zonal velocities are of similar magnitude, implying that the mean deep zonal flow field is significantly different from synoptic snapshots (middle panel). Additionally, the unsteady flows in the model do not dominate synoptic snapshots either and there are regions where the synoptic model velocities agree well

with tracer distributions (e.g. Figure 1). This is consistent with the generally ambiguous conclusions resulting from comparisons of tracer fields and synoptic geostrophic velocities discussed above. Again in agreement with the data-based inference, the meridional scales of the unsteady flow field at depth are of the same order as those of the mean circulation. Therefore, it is not possible to use horizontal averaging to separate the mean from the unsteady zonal flows at depth in the Brazil Basin, at least not without knowledge of the spatial distribution of the relevant scales.

Traditionally, oceanic flows are often determined by adding reference velocities to geostrophic profiles derived from synoptic sections. When the results are interpreted to represent more than temporal snapshots (e.g. whenever multiple data sets are combined) the large-scale time-varying velocities are assumed to be either barotropic or weak in comparison to the time-mean circulation. While this is often a good assumption for the near-surface circulation we have used hydrographic data and output from a numerical model to show that it is violated in the deep interior of the Brazil Basin.

If eastward zonal transport of NADW across 25°W represents export from the southward flowing Deep Western Boundary Current (including recirculations) on the continental slope (8) the unsteady contribution (bottom panel of Figure 3) violates the volume-conservation assumption of linear box-inverse models applied to zonal synoptic sections occupied at different times and will lead to errors in the meridional transports of heat and other properties. The magnitude of the unsteady contribution to the zonal NADW transport shown in Figure 3 (using 1200 m and 3700 m as upper and lower limits (16)) between 11° and 19°S (the latitudes of two zonal WOCE sections) is $>5\text{ Sv}$, or approximately 25% of the total southward NADW transport (8) and much larger than typical *a priori* errors assumed in box inversions (1). In order to determine the mean deep circulation in the interior of the Brazil Basin (and probably in other regions as well) from hydrographic sections, inverse models that can adjust the density field or that are explicitly time-dependent (21) must be used. The difference in vertical structure of the mean and the unsteady zonal flow fields in the Brazil Basin provides an indication how improved inverse models can

be constructed. The observation that the mean zonal circulation has a clear signature in synoptic density-gradient sections is furthermore extremely useful for testing numerical models, for example those used for climate simulations (22) and ocean-state estimations (21), as well as for the design of future field programs.

References

- [1] C. Wunsch, *The Ocean Circulation Inverse Problem*, (Cambridge University Press, 1996).
- [2] G. Siedler, J. Church, J. Gould, Eds., *Ocean Circulation & Climate*, (Academic Press, 2001).
- [3] N. G. Hogg, W. B. Owens, *Deep Sea Res. II* **46**, 335 (1999).
- [4] N. G. Hogg. Quantification of the deep circulation. in *Ocean Circulation & Climate*, G. Siedler, J. Church and and J. Gould, Eds. Academic Press, (2001), pp. 259–270.
- [5] M. Tsuchiya, L. D. Talley, M. S. McCartney, *J. Mar. Res.* **52**, 55 (1994).
- [6] J. L. Reid, *Prog. Oceanogr.* **23**, 149 (1989).
- [7] H. M. Zhang, N. G. Hogg, *J. Mar. Res.* **50**, 385 (1992).
- [8] X. D. DeMadron, G. Weatherly, *J. Mar. Res.* **52**, 583 (1994).
- [9] L. Stramma, M. England, *J. Geophys. Res.* **104**, 20863 (1999).
- [10] A new WOCE-period hydrographic and tracer climatology of the South Atlantic; see <http://www.ocean.fsu.edu/SAC> for details.
- [11] A.-M. Treguier, N. G. Hogg, M. Maltrud, K. Speer, V. Thierry, *J. Phys. Oceanogr.* (*in press*) (2002).
- [12] J. Lupton, *J. Geophys. Res.* **103**, 15853 (1998).
- [13] G. Wüst, *Wissenschaftliche Ergebnisse der Deutschen Atlantischen Expedition auf dem Forschungs- und Vermessungsschiff "Meteor" 1925–1927* **6**, 180pp (1935). Reprinted as *The Stratosphere of the Atlantic Ocean*, W.J. Emery (ed.), 1978, Amerind, New Delhi, 112pp.
- [14] C. Wunsch. Global problems and global observations. in *Ocean Circulation & Climate*, G. Siedler, J. Church and and J. Gould, Eds. Academic Press, (2001), pp. 47–58.

- [15] L. Armi, H. Stommel, *J. Phys. Oceanogr.* **13**, 828 (1983).
- [16] M. Vanicek, G. Siedler, *J. Phys. Oceanogr.* **32**, 2205 (2002).
- [17] A. M. Thurnherr, K. G. Speer, *J. Phys. Oceanogr.* (*in press, available at <ftp://cookymouse.ocean.fsu.edu> in directory /pub/submitted*) (2002).
- [18] T. Suga, L. D. Talley, *J. Geophys. Res.* **100**, 13441 (1995).
- [19] $u_z = g/(f\rho_0)\rho_y$, where u_z is the vertical shear of the geostrophic zonal velocity, g the acceleration due to gravity, f the Coriolis parameter, ρ_0 a reference density, and ρ_y the meridional gradient of density. E.g. Gill, A. E. *Atmosphere-Ocean Dynamics*. Academic Press, (1982).
- [20] The model is initialized with climatology and spun up for 18 years, first with an ECMWF-derived repeated annual cycle for 8 years and then with daily winds. After spinup it is dynamically (but not thermodynamically) adjusted because the first 6 baroclinic normal modes have had time to cross the entire Brazil Basin (3000 km) at 11°S.
- [21] L. D. Talley, D. Stammer, I. Fukumori. Towards a WOCE synthesis. in *Ocean Circulation & Climate*, G. Siedler, J. Church and J. Gould, Eds. Academic Press, (2001), pp. 525–545.
- [22] C. W. Böning, A. J. Semtner. High-resolution modelling of the thermohaline and wind-driven circulation. in *Ocean Circulation & Climate*, G. Siedler, J. Church and J. Gould, Eds. Academic Press, (2001), pp. 59–77.
- [23] ACKNOWLEDGMENTS. We thank the contributors of the hydrographic data sets used in this study. J. Zavala provided valuable comments on the manuscript. The analysis was carried out in the context of the WOCE AIMS Deep Basin Experiment Synthesis project (NSF grant OCE-9911148). Contribution to the World Ocean Circulation Experiment.

Figure 1: Bias-corrected (10) oxygen field (shading and contours) and float velocities (blue arrows) at 2500 m in the Brazil Basin. Dots show station positions; warm colors indicate high oxygen concentrations; contour level is $2.5 \mu\text{mol}\cdot\text{kg}^{-1}$; gray areas without contours are shallower than 2500 m. The solid line near 14°W shows the crest of the Mid-Atlantic Ridge. The float-derived velocities are taken from Fig. 9 of a recent study by Treguier et al. (11) and show spatially averaged values (2° of latitude by 8° of longitude); zonal-velocity uncertainties are indicated at the tips of the arrows; none of the meridional velocities are distinguishable from zero (11).

Figure 2: Meridional density gradients in the Brazil Basin, in units of $\text{kg}\cdot\text{m}^{-4}$. (a) and (b): from linear fits to hydrographic observations in 7.25° -wide meridional windows; the horizontal line in panel (b) near 4000 m shows the extent of the observations at 19°W . (c): from the hydrography of a high-resolution numerical model (11).

Figure 3: Zonal model flows in the Brazil Basin, horizontally smoothed with a 2.5° Gaussian filter. (a) Mean flow in modeling period 1989–1994. (b) Snapshot. (c) Unsteady residual (snapshot minus mean).

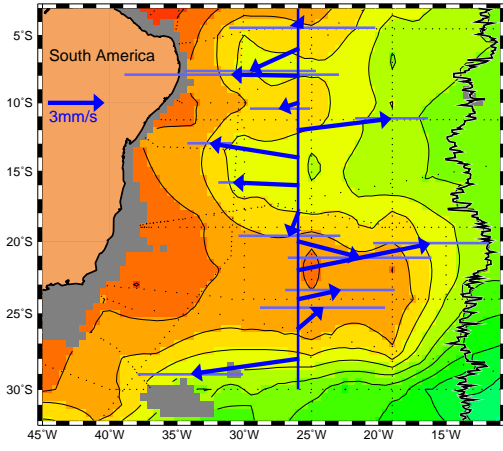


Figure 1.

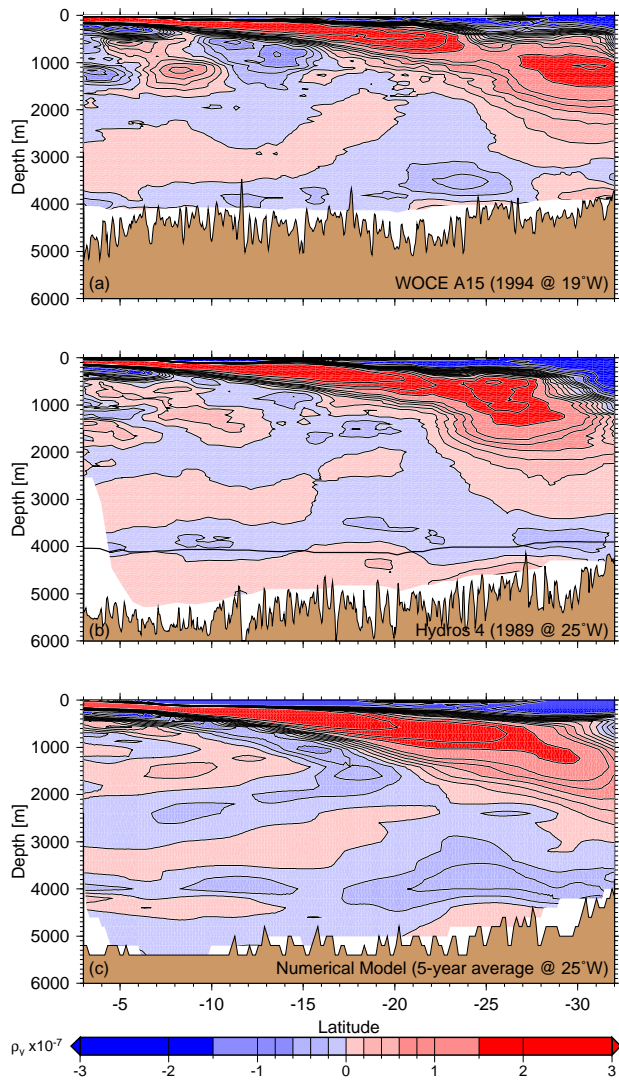


Figure 2.

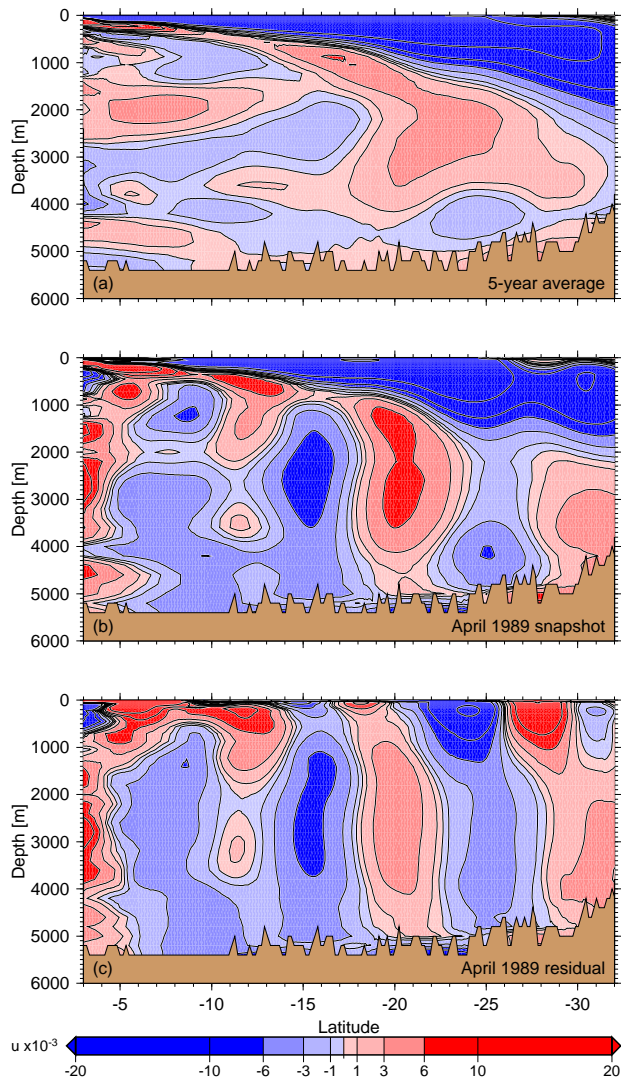


Figure 3.